JOURNAL OF SOLID STATE CHEMISTRY **129,** 82–91 (1997)
ARTICLE NO. SC967234

Cation Sublattice and Coordination Polyhedra in ABO_4 Type of Structures

Laura E. Depero* and Luigi Sangaletti†

*Dipartimento di Chimica e Fisica per i Materiali and †Istituto Nazionale di Fisica per la Materia, Universitat Brescia, Via Branze 38, 25123 Brescia, Italy

Received June 24, 1996; in revised form November 13, 1996; accepted November 18, 1996

The common features of the ABO_4 type of structures are reviewed and discussed. A preliminary statistical study of the distribution of the space group for these compounds is proposed and the similarities and differences among the structure types are discussed. Using the recently proposed approach for structural study (L. E. Depero and L. Sangaletti, *J. Solid State Chem.* 119, 428 (1995)), the cation sublattices of these structures are compared and described as a continuous transformation from the space group no. 216, in which the coordination number of the cation is 12, to the rutile and the α-PbO_2 structures, where the coordination number is 6. In this approach, the phase transformation of the polymorphic phases, largely present in this family, can be understood in terms of changes in the cation sublattice.

INTRODUCTION

The study of analogies and differences among structures belonging to the same type may help to determine the factors involved in the structure stability and, therefore, to design new structures or discuss structural changes in polymorphic phases. Moreover, the influence of the cation on the crystal structure can help in modeling the effect of impurities on the physical properties. Indeed, the development of laser crystal physics is strictly related to the structural characterization of materials, usually insulating oxides doped with trivalent rare earth (*RE*) cations. Among these *RE* activated crystals, simple and mixed oxide crystals are found belonging to the ABO_4 type of structure (1). This is the case, for example, of laser crystals based on yttrium vanadate (YVO_4), where cationic impurities are introduced in the host crystal to obtain laser light emission at desired frequencies (2).

In the case of mixed disordered systems (solid solutions), Re^{3+} ions are distributed over many activator centers with different coordinations. Hence, the absorption spectra of these materials consist of strong broad lines which provide much better utilization of pump power (see, e.g., Table 1.4 in Ref. (1)).

In both cases, the *RE* coordination strongly affects the emission properties of the crystal. Therefore, a study of structural distortions in cation coordination can provide useful information to address the crystal growth and better understand the fine structure of the emission lines.

In recent years, the comparison among crystal structures has been promoted to a considerable extent by the high accuracy in the determination of the positions of the atoms achieved in the structural analysis of single crystals and by the creation of an extensive and rapidly increasing stock of experimental data. These facts create favorable conditions for far-reaching theoretical generalizations.

The aim of this work is to review the common ABO_4 type of structures and to find analogies and differences among them and with respect to the rutile and α-PbO_2 type of structures. The following issues will be discussed:

(i) statistical distribution of ABO_4 compounds in space groups;

(ii) distribution of the average distances between *A* and *B* cations and oxygen and their relationship with the distortion of coordination polyhedra;

(iii) discussion of the relationship among zircon, rutile, wolframite, and α-PbO_2 structures. These structures are the most common structural types in the ABO_4 family. The ABO_4 compounds can therefore be discussed in the frame of structural relations among these four prototypes.

The building block of both rutile and α-PbO_2 structures is the $[AO_6]^{8-}$ octahedron. The difference between the two structures can be evidenced by looking at the chain of edge-sharing octahedra. In the case of rutile, the edge-sharing octahedra chains run parallel to the [001] direction, while in the α-PbO_2 phase the chains run in a zigzag fashion. Indeed, the α-PbO_2 structure can be described as the rutile phase with twinning planes orderly distributed along the lattice to give the zigzag chains in the [100] direction (3). The structural correlation between these two phases has been recently discussed (4) and their structural properties have been related to the electronic structure in a recent study (5). On the basis of this discussion, also the formation of such systems as $FeNbO_4$–TiO_2 (6), where not

0022-4596/97 $25.00

only a rutile type but also a wolframite type solid solution exists, can be carried out.

(iv) Comparison of the structures in terms of coordination polyhedra networks as well as in terms of atom distribution in the cation sublattice.

Indeed, there has been some tendency to consider polyhedra networks as rigid structures. Cubic MoO_3 networks based on MoO_6 octahedra may be taken as an example. The linking of these octahedra gives the highly flexible perovskite structure if the cubic symmetry is lowered to tetragonal and orthorhombic (7). Recently, it was suggested to explore the networks flexibility with simulations using the distance least squares (DLS) program, a well-known approach to refine structures based on prescribed distances (8). In particular it was shown that for analcite, high flexibility requires relaxing the ideal symmetry and high pressure should induce lower symmetry structure (9). In the present work an alternative approach is proposed to discuss the flexibility of the ABO_4 structures, based on analysis of the cation distribution in the lattice.

DISCUSSION

In this study, the Inorganic Crystal Structure Database (ICSD) (10) has been used to select the crystal structures and the modeling has been performed by the CERIUS program (11).

In Fig. 1, the distribution of the space groups in the ABO_4 compounds is shown. The dataset (reported in the Appendix) has been selected by choosing ABX_4 structures containing oxygen. To this dataset, the disordered structures isomorphous to rutile or α-PbO_2 containing two cations disordered in the same sites were added. Most of the structures (62%) belong to one of the following space groups: nos. 13, 14, 15, 60, 62, 88, 136, 141, and no. 216. It has been verified that, with few exceptions, structures with the same space group (SG) and similar cell volume are isostructural. It is generally true that, in the same SG, isostructural compounds have the same Wykoff positions, even if, in few cases, the conventional unit cell is not used, and, consequently, isostructural compounds can have different Wykoff positions.

It is common to relate the coordination number (CN) of the A and B cations and, consequently, the type of crystal structure, to their ionic radii (12). In qualitative terms, it is commonly accepted that "small" cations lead to low CN, while "large" cations have large CN (13). In this approach, the coordination number of A cation in $CsClO_4$ (CN = 12, SG no. 216), $PbCrO_4$ (CN = 10, SG no. 62), $CaCrO_4$ (CN = 8, SG no. 141), and $CdWO_4$ (CN = 6, SG no. 13) are justified.

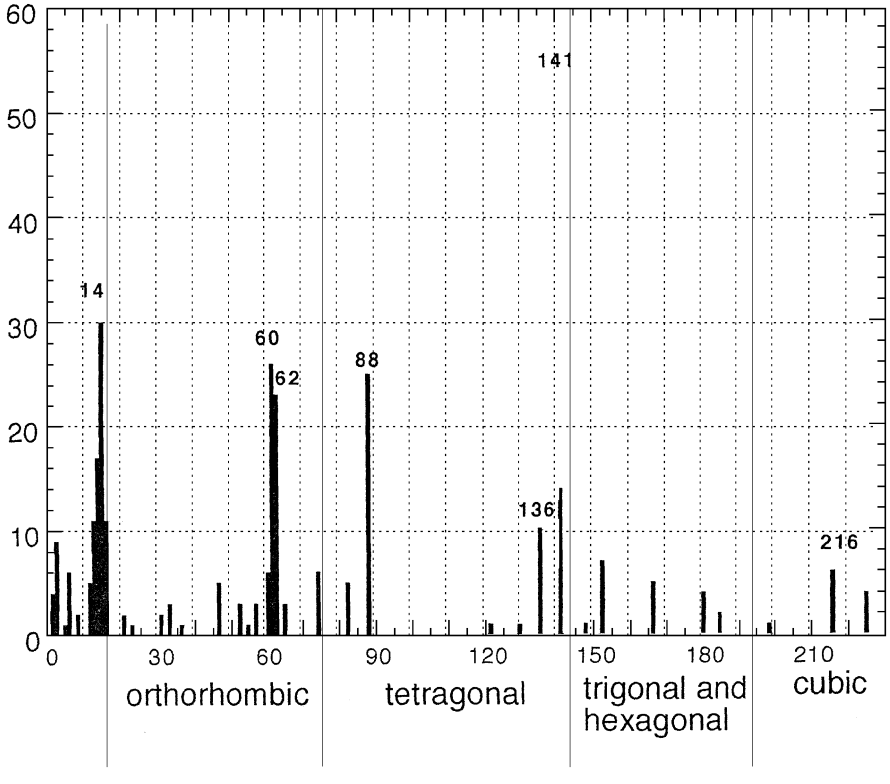

FIG. 1. The statistical distribution of the ABO_4 structures against the SG number (see also Appendix).

However, for the discussion of the several polymorphic phases found in the database, additional parameters seem to be necessary. Indeed, in view of the possibilities of obtaining for a given cation the same oxidation state in different coordinations, it is necessary to describe its coordination by introducing, at least, two parameters: the *A*–O and *B*–O average distances [$d_a(A\text{–O})$ and $d_a(B\text{–O})$] in the coordination polyhedra and the standard deviation of the *A*–O coordination from the average distance, which is related to its distortion.

In Fig. 2a the distribution of the average distance $d_a(A\text{–O})$ and $d_a(B\text{–O})$ for the ABO_4 structures is shown for all the considered space groups. The percentiles of the distributions are indicated. The $d_a(A\text{–O})$ distance is largest in structures belonging to SG nos. 216 and 62 ($BaSO_4$ type), $d_a(A\text{–O})$ is constant at about 2.5 Å for structures belonging to SG nos. 14, 141, and 88, and is smaller than 2.5 Å for SG nos. 15 and 60. For SG no. 13 (wolframite) the average value of the $d_a(A\text{–O})$ and $d_a(B\text{–O})$ is close to 2.1 Å. Similar values are obtained for ABO_4 structures in SG no. 136 (corresponding to disordered rutile type of structure).

In Fig. 2b the distribution of the $d_a(B\text{–O})/d_a(A\text{–O})$ ratios is shown. The average values for this ratio can be grouped into three types: SG nos. 216 and 62, with average value of about 0.55, SG nos. 14, 141, 88, with average value of about 0.7, and the SG nos. 15, 60, and 13 where the average value is larger than 0.9. However, the large dispersion in the distribution of these ratios in the different space groups shows that, beside the average distance in the distribution, the distortion of the coordination must be accounted for as a parameter determining the crystal structure SG.

In the SG nos. 216, 62, 14, 141, and 88, where the average of *B*–O average distance is less than 1.8 Å, the coordination polyhedra of *B* is a tetrahedron, while for the other considered SG the *A* and *B* polyhedra are both octahedra. The larger dispersion of the average distance distribution found for the SG no. 62 can be justified by the fact that the CN of the *A* cation can vary from 12 to 8. In Fig. 2c the distribution of the standard deviation of the *A* coordination is shown. For SG no. 216 the standard deviation of the distribution is zero, since, by symmetry, all the distances are the same. For the SG no. 62, even though the average standard deviation of the coordination is small (about 0.1), a large dispersion is found for its distribution. This fact confirms that in the SG no. 62 large distortions of the *A* polyhedra are possible, allowing the CN of *A* to vary, as observed above. The highest standard deviation (0.32) is found for SG no. 15, even though the corresponding structure is closely related to SG nos. 88 and 141. The high value of the average of the $d_a(B\text{–O})/d_a(A\text{–O})$ ratio, as well as the high average of the standard deviation for the structures in SG no. 15 is justified by considering that two bonds became very long, resulting in CN = 6 + 2, instead of CN = 8). Indeed, the structures of SG no. 15 are very similar to those of SG no. 141, except that a large distortion in *A* coordination is usually found.

The relationships among the considered space groups correspond also to group–subgroup relationships found

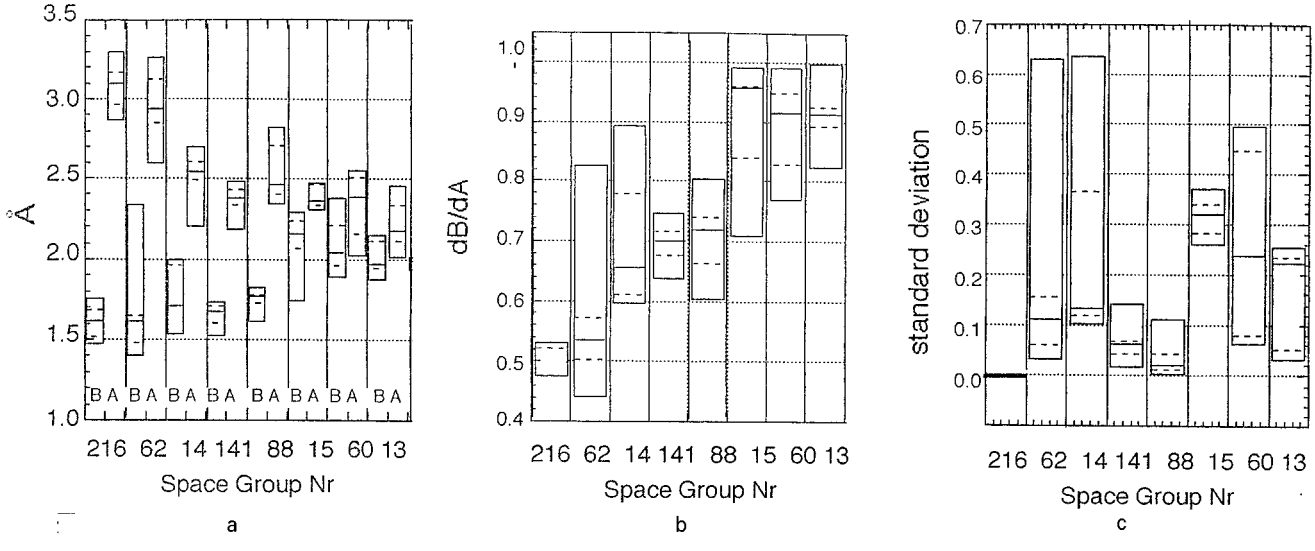

FIG. 2. (a) Average distances $d_a(B\text{–O})$ and d_a $(A\text{–O})$ of the coordination of *B* and *A* cations for the considered SGs. (b) Ratio d_a $(B\text{–O})/d_a(A\text{–O})$ between the average distance of the *B*–O coordination and the average distance of the *A*–O coordination. (c) Standard deviation of the *A* coordination from the average d_a distance.

among them, in particular:

$$14 \subset 62;\ 15 \subset 88 \subset 41;\ 13 \subset 60.$$

The zircon and the rutile structures are closely related (3). This relationship can be appreciated from an inspection of Fig. 3, where proper view of the rutile (Figs. 3a and 3b), YVO_4 (Figs. 3c and 3d) and $BiVO_4$ (Figs. 3e and 3f) crystal structures are shown. In this view the cation of the zircon and rutile structures are coincident, the only difference being the positions of the oxygen ions (small circles), which

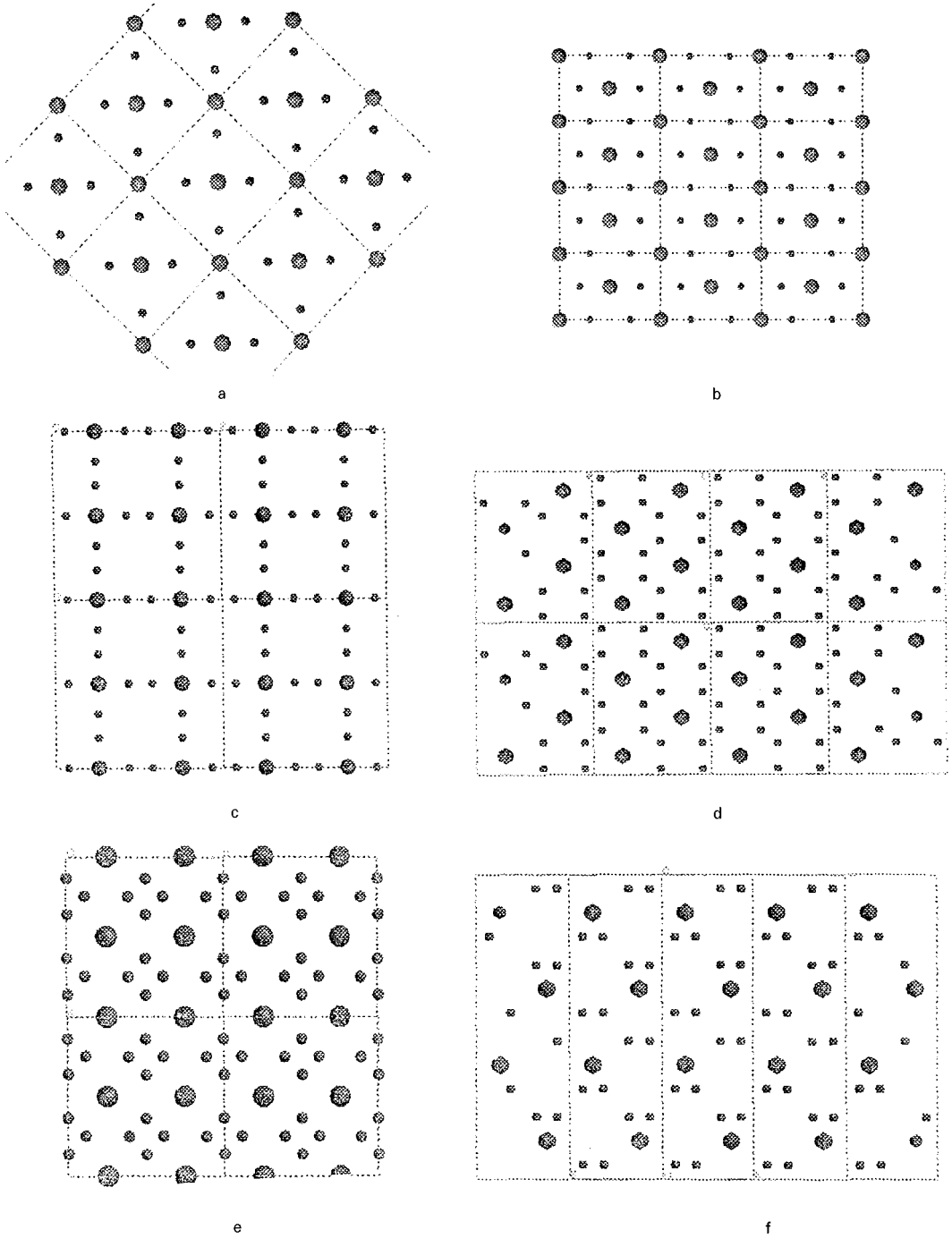

FIG. 3. Projection of the rutile structure parallel to [001] (a) and to [100] (b); projection of the YVO_4 structure (SG 141) parallel to [001] (c) and to [110] (d); projection of the $BiVO_4$ structure (SG 88) parallel to [001] (e) and to [110].

allows, in the case of YVO_4 , CN = 8 for the *A* cation and CN = 4 for the *B* cation, while CN = 6 for both *A* and *B* cations in rutile.

In Figs. 3e and 3f the same comparison has been done for structures belonging to SG no. 88. As an example, the structure of $BiVO_4$ is considered. The cation positions are coincident with those of the rutile also in this structure, while the oxygen ions in the *ab* plane are differently distributed (Figs. 3a, 3c, and 3e). On the contrary, the oxygen distribution in the plane containing the *c* axes is similar (Figs. 3b, 3d, and 3f).

Wolframite and α-PbO_2 are isostructural, the only difference being the ordering of the cation in the cation sites of the wolframite structure.

ABO_4 compounds belonging to the rutile (SG no. 136) and α-PbO_2 type of structure (SG no. 60) are found only in the case of disorder in the cation sublattice.

In Fig. 4 the coordination polyhedra of the *B* atom in ABO_4 in some of the considered space groups are shown. As shown in Fig. 4a, the distribution of the polyhedra of *B* in SG no. 216 is different from that of all of the other structures. While the coordination polyhedra are found in couples distributed on a pseudo-hexagonal network in the structures reported in Figs. 4b–4f, in the case of Fig. 4a only a single tetrahedron is found at the points of the pseudo-hexagonal network. Focusing on the tetrahedra couples, it is possible to appreciate the transition from the arrangement in SG no. 62 (Fig. 4b) to SG no. 88 (Fig. 4e), through SG nos. 14 (Fig. 4c) and 141 (Fig. 4d). In the case of SG no. 60 (Fig. 4f) the packing of the oxygen is different, giving rise to a different orientation of the tetrahedra.

The comparison of the structural properties of complex oxides in terms of coordination polyhedra may be a difficult task due to the different coordination of metal cations with oxygen. A new approach was recently proposed for the structural study of inorganic compounds based on the search of the common features detectable in the cation sublattice distribution and applied to the Mo–Bi–O ternary system (14). In this frame, the different metal sublattice of the type of structures in the ABO_4 family are compared in Fig. 5. It is possible to observe a continuous evolution from the cubic structure of $BaSO_4$ (SG no. 216, Fig. 5a) to zircon structure (SG no. 141, Fig. 5d). The evolution of the cation lattice corresponds to a change in the CN of the *A* cation from 12 (SG no. 216) to 8 (SG no. 141) passing through 10 (SG no. 62). As in the case of the Bi–Mo–O oxides (14), the cation lattice seems to control the crystal structure. Indeed, as recently discussed (15), the cation–cation repulsions, in addition to the bond network, are able to direct the distortion in the case of the octahedrally coordinated d° transition metal, while other effects, such as lattice stress and electronic distortion, show no directional preferences.

Focusing on the atom distribution in the cation sublattice, it is possible to discuss the ABO_4 structures from the cubic (SG no. 216, with the CN of *A* equal to 12) to the wolframite. The cation sublattice of structures with SG no. 88 is the same as that of Fig. 5d. In the figure, two perpendicular *A*–*B*–*A*–*B*–..... chains are shown and the changes in the different structures can be easily seen. In all of the structures one chain remains straight, while the second has a still zigzag conformation and remains perpendicular to the first in SGs nos. 62, 14, 141, 15. In wolframite, the chains are both straight, but the angle between them is $\neq 90^\circ$.

CONCLUSION

Even if different polyhedra networks are found in ABO_4 structures, it was observed that strong similarities can be identified in the cation sublattices. The proposed approach can be useful in discussing the changes among polymorphic phases, such as in the case of phase transformations.

For example, in the case of $BiVO_4$ polymorphs, the Bi coordination geometry can be significantly different. The change of the coordination can be tentatively ascribed to a change in the electronic density around the Bi atoms. In particular, the presence of electron lone pair in the external shell of the Bi can determine the polymorphism of $BiVO_4$. Indeed, at high temperature the occupation of the *s* orbital from these electrons can be favored, resulting in a more symmetrical distribution, while, at RT the occupation of localized orbital may induce a strong distortion, as that found in the structure $BiVO_4$ belonging to SG no. 60.

The proposed discussion can also be applied to the case of a ABO_4 structure with more than two cations statistically distributed in the cation sites, as in the case of $Pb_{0.5}Th_{0.5}VO_4$, which presents three polymorphs in SGs nos. 88, 141, and 14 (16). In all of these structures, the cation sublattice is that found in rutile, while the differences must be attributed to the oxygen sublattice.

A global view of the relationship among structures is particularly useful in the study of, e.g., pressure-induced phase transitions. In the case of $CdWO_4$, a first transition at a 12 GPa from the scheelite (SG no. 88) to the wolframite phase is observed, while a second phase transition occurs at $\sim$ 25 GPa (17, 18). Similar transformations were found by Raman spectroscopy studies on $CaMoO_4$, at 8.2 and 15 GPa (19). Also in this case, the behavior is related to the increase in the coordination number of the Mo ion in the high-pressure phases. In the scheelite type $SrMoO_4$, transformation into a monoclinic lattice near 13 GPa is observed (20), which can probably be related to similar phase transition mechanisms. Indeed, also for $CoMoO_4$ and $NiMoO_4$ the wolframite structure has been observed at high pressures (21).

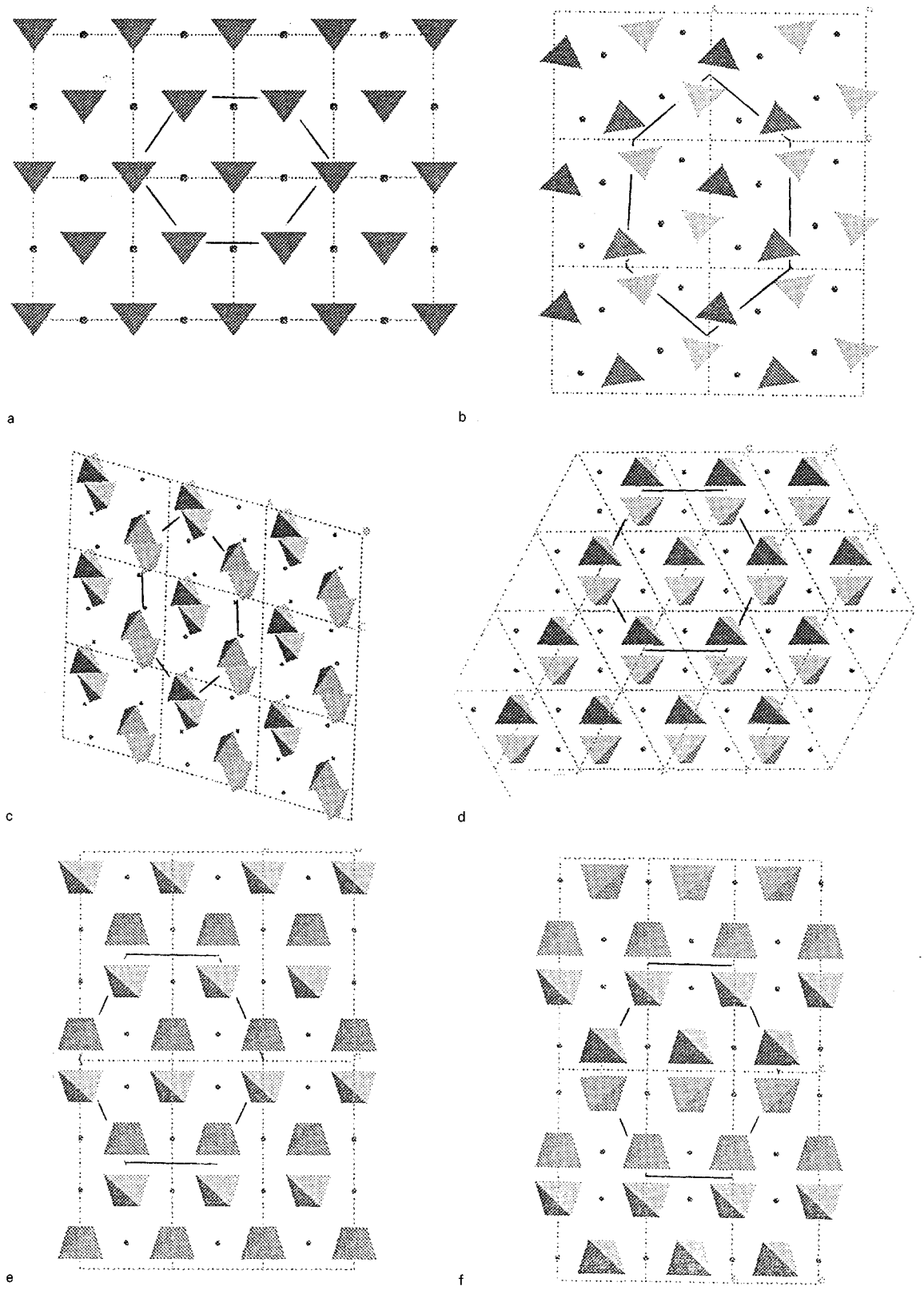

FIG. 4. View of the *B* coordination tetrahedra in $BaSO_4$, SG 216 (a) and SG 62 (b); $BiPO_4$, SG 14 (c); $BiVO_4$, SG 141 (d), SG 88 (e), and SG 60 (f).

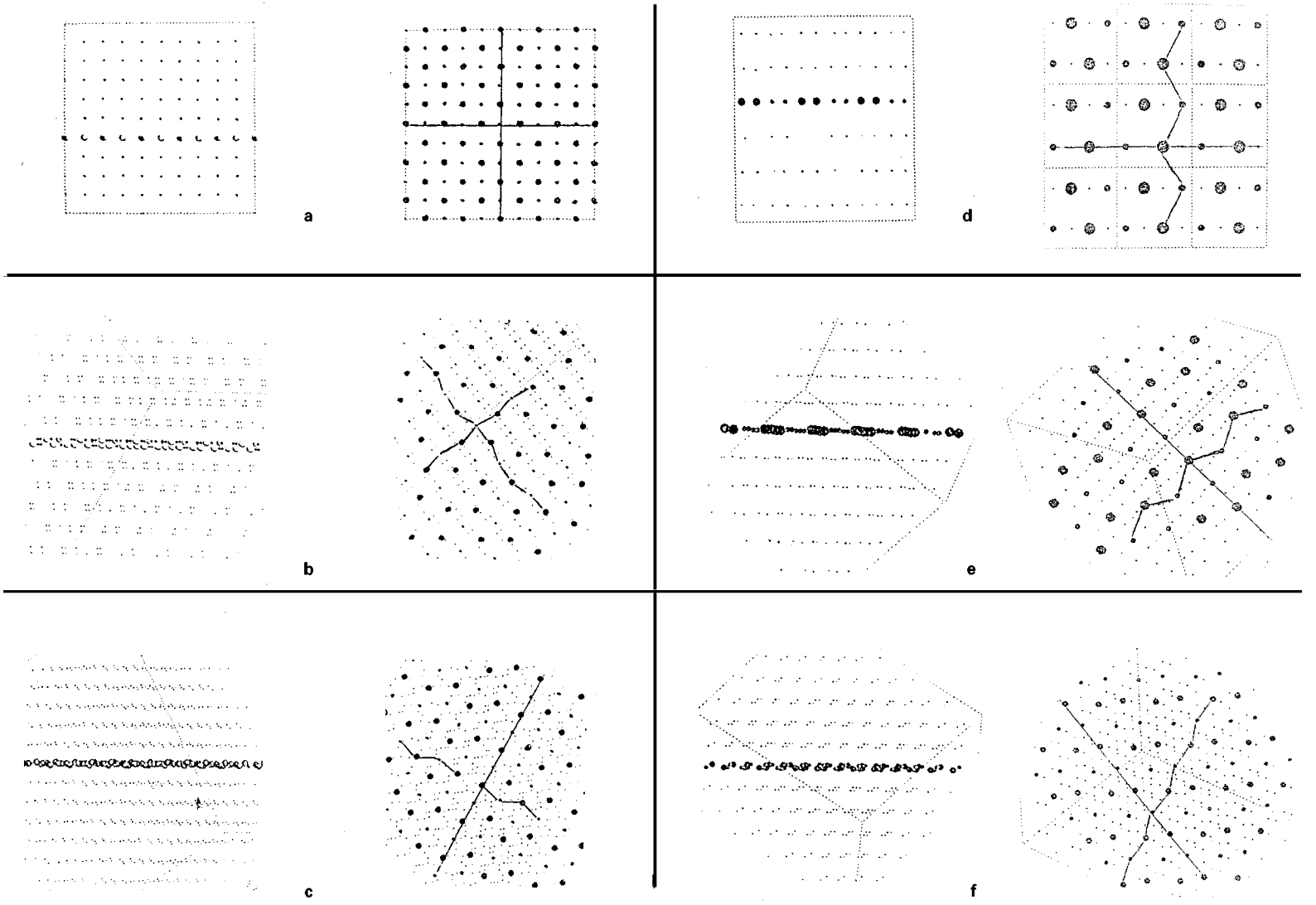

FIG. 5. View, orthogonal and parallel to the indicated directions, of the cation sublattice in the more representatives ABO_4 structures: (a) $BaSO_4$, SG 216, [001] direction; (b) $BaSO_4$, SG 62, [210] direction; (c) $BaPO_4$, SG 14, [120] direction; (d) YVO_4, SG 141, [100] direction; (e) $BiVO_4$, SG 15, [112] direction; (f) wolframite, SG 13, [111] direction. For rutile and for structures with SG 88 a pattern similar to (d) is obtained, while for structures with SG 60. a pattern similar to (f) is obtained.

APPENDIX

ABO_4 Phases Found in the Inorganic Crystal Structure Database

Col	Formula	Cell	Cell volume	SG no.	Wykoff positions
100280	**$AgClO_4$**	**1/1.36**	**167.0**	**121**	*i b a*
33568	**$AgClO_4$**		**331.4**	**216**	*e b a*
31429	**$AgClO_4$**		**347.4**	**225**	*j b a*
36072	$AgMnO_4$	1/1.48/1.26	334.2	14	*e* 6
24512	**$AlAsO_4$**	**1/1.36**	**159.4**	**82**	*g d a*
33832	**$AlAsO_4$**	**1/2.23**	**245.8**	**152**	*c2 b a*
20342	$AlNbO_4$	1/0.31/0.53	280.5	2	*i*6
67498	**$AlPO_4$**	**1/1.65/0.39**	**1577.6**	**2**	*i* 1 8
71435	**$AlPO_4$**	**1/0.93/1.35**	**3241.7**	**15**	*f* 1 8
16651	**$AlPO_4$**	**1/0.99**	**353.1**	**20**	*c2 b a*
74462	**$AlPO_4$**	**1/0.44/0.25**	**4106.0**	**36**	*b25 a4*
63664	**$AlPO_4$**	**1/1.37/0.62**	**2093.7**	**46**	*c13 b4*
24511	**$AlPO_4$**	**1/1.36**	**155.2**	**82**	*g d a*
72374	**$AlPO_4$**	**1/0.24**	**1879.4**	**148**	*f*6
33742	**$AlPO_4$**	**1/2.21**	**231.3**	**152**	*c2 b a*
68933	**$AlPO_4$**	**1/0.43**	**2533.5**	**185**	*d7 c4*
33885	**$AlTaO_4$**	**1/0.31/0.53**	**281.5**	**12**	*i*6
67676	**$AlTaO_4$**	**1/2.53/1.07**	**241.5**	**60**	*d2 c2*
35642	**$AlTaO_4$**	**1/0.65**	**63.3**	**136**	*f a*
4164	$AlWO_4$	1/0.63/0.5	234.8	12	*j i3 g*
31879	$AsPO_4$	1/0.6/0.85	305.1	62	*d c4*
23316	$AsSbO_4$	1/1.44/1.11	175.8	11	*f e4*
10436	$As2O_4$	1/0.61/0.85	327.1	62	*d c4*
26891	$BAsO_4$	1/1.52	135.1	82	*g c a*
26890	BPO_4	1/1.53	124.6	82	*g c a*
62560	$BaCrO_4$	1/0.61/0.81	369.6	62	*d c4*
16166	$BaMoO_4$	1/2.28	404.9	88	*f2 b a*
33730	**$BaSO_4$**	**1/0.61/0.81**	**343.3**	**62**	*d c4*
62368	**$BaSO_4$**		**407.7**	**216**	*e b a*
36239	$BaUO_4$	1/1.41/1.43	385.3	57	*e d2 c a*
2144	**$BaWO_4$**	**1/0.54/0.57**	**705.1**	**14**	*f*12
23702	**$BaWO_4$**	**1/2.27**	**400.8**	**88**	*f b a*
16832	$BeSO_4$	1/1.54	139.1	82	*g c a*
27199	**$BiAsO_4$**	**1/1.04/0.98**	**320.5**	**14**	*e*6
30636	**$BiAsO_4$**	**1/2.3**	**301.9**	**88**	*f b a*
10247	**$BiNbO_4$**	**1/0.73/1.04**	**325.2**	**2**	*i* 12
62132	$CrAsO_4$	1/0.7/0.53	265.6	62	*d c3 a*
27943	$CrNbO_4$	1/0.65	64.9	136	*f a*
62159	**$CrPO_4$**	**1/1.5/1.18**	**245.4**	**63**	*g f c a*
63153	**$CrPO_4$**	**1/1.24/0.61**	**840.3**	**74**	*j2 i h g2 e*
72276	$CrTaO_4$	1/0.65	65.1	136	*f a*
202755	$CrVO_4$	1/1.48/1.07	276.4	63	*g f c a*
8269	**$CrWO_4$**	**1/0.63/0.5**	**250.4**	**12**	*j i3 g*
36213	**$CrWO_4$**	**1/0.97/0.44**	**1002.4**	**22**	*k2 j3 i h f2*
201158	**$CsBrO_4$**	**1/2.58**	**490.2**	**88**	*f b a*
73299	**$CsBrO_4$**	**1/2.58**	**490.2**	**141**	*h b a*
63364	**$CsClO_4$**	**1/0.61/0.79**	**458.3**	**62**	*d c4*
33566	**$CsClO_4$**		**504.4**	**216**	*e b a*
31430	**$CsClO_4$**		**519.7**	**225**	*f b a*
16819	$CsMnO_4$	1/0.58/0.79	464.8	62	*d c4*
74505	**$CsReO_4$**	**1/1.04/2.49**	**493.9**	**62**	*d c4*
72817	**$CsReO_4$**	**1/2.42**	**513.3**	**141**	*h b a*
67884	CsSO3F	1/2.52	450.3	41	*h b a*
39540	$CsTcO_4$	1/1.03/2.5	486.3	62	*d c5*
60825	$CuCrO_4$	1/1.65/1.08	287.0	63	*g f c a*
39439	**$CuMoO_4$**	**1/1.03/1.24**	**133.5**	**2**	*i*6
22276	**$CuMoO_4$**	**1/0.68/0.84**	**517.4**	**2**	*i*18
71017	$CuSO_4$	1/0.8/0.57	272.7	62	*d c3 a*
1672	$CuTeO_4$	1/1.88/0.86	267.2	14	*e5 d a*
36071	$CuUO_4$	1/0.91/1.2	156.1	14	*e2 c a*
24339	$CuWO_4$	1/1.24/1.04	132.7	2	*i*6
200229	**$DyAsO_4$**	**1/1/0.89**	**312.2**	**74**	*i h e2*
200228	**$DyAsO_4$**	**1/0.89**	**314.5**	**141**	*h b a*
26984	$DyCrO_4$	1/0.88	320.1	141	*h b a*
35705	$DyPO_4$	1/0.88	288.4	141	*hba*
20263	$DyTaO_4$	1/1.03/0.96	148.4	13	*g2 f e*
26441	$DyVO_4$	1/0.88	321.2	141	*h b a*
26986	$ErCrO_4$	1/0.88	313.4	141	*h b a*
36052	$ErPO_4$	1/0.88	282.5	141	*h b a*
20262	$ErTaO_4$	1/1.03/0.96	146.0	13	*g2 f e*
69118	**$ErVO_4$**	**1/2.23**	**278.9**	**88**	*f b a*
15671	**$ErVO_4$**	**1/0.88**	**316.5**	**141**	*h b a*
26981	$EuCrO_4$	1/0.88	330.2	141	*h b a*
201840	$EuPO_4$	1/1.03/0.95	277.7	14	*e*6
68244	$EuSO_4$	1/0.64/0.82	308.8	62	*d c4*
15608	$EuVO_4$	1/0.88	329.2	141	*h b a*
73978	$FeAsO_4$	1/1.07/0.66	296.5	14	*e*6
14016	**$FeNbO_4$**	**1/0.31/0.53**	**290.6**	**2**	*i*6
14015	**$FeNbO_4$**	**1/1.12/0.93**	**129.8**	**13**	*g2 f e*
203006	**$FeNbO_4$**	**1/1.21/1.08**	**130.8**	**60**	*d c*
201795	$FePO_4$	1/2.23	245.9	152	*c2 b a*
23507	$FeSO_4$	1/1.52/1.25	276.1	63	*g f c a*
9517	$FeTaO_4$	1/0.65	66.7	136	*f a*
24963	$FeUO_4$	1/2.44/1.05	298.2	60	*d2 c2*
10329	$FeVO_4$	1/1.2/1.38	462.5	2	*i*18
26843	$FeWO_4$	1/1.21/1.05	133.6	13	*g2 f e*
33256	$GaAsO_4$	1/2.28	245.4	152	*c2 b a*
18187	$GaNbO_4$	1/0.3/0.52	302.2	5	*c*6
16652	**$GaPO_4$**	**1/0.99**	**333.3**	**20**	*c2 b a*
62850	**$GaPO_4$**	**1/2.25**	**229.7**	**152**	*c2 b a*
72570	$GaTaO_4$	1/1.21/1.08	128.2	60	*d c*
26982	$GdCrO_4$	1/0.88	327.7	141	*h b a*
20408	$GdNbO_4$	1/2.1/0.99	305.1	46	*c2 b2*
20421	$GdNiO_4$	1/2.06/0.95	303.5	5	*c2 a2*
201841	$GdPO_4$	1/1.03/0.95	276.4	14	*e*6
20264	$GdTaO_4$	1/1.03/0.96	151.4	13	*g2 f e*
15607	$GdVO_4$	1/0.88	327.2	141	*h b a*
16639	$GeUO_4$	1/2.21	290.2	88	*f b a*
202080	$HfGeO_4$	1/2.16	248.1	88	*f b a*
59111	$HfSi_4$	1/0.91	258.9	141	*h b a*
27028	$HfTiO_4$	1/1.18/1.07	135.4	60	*d c*
2224	$HgCrO_4$	1/1.16/0.71	324.7	14	*f*6
2533	$HgMoO_4$	1/0.54/0.46	325.8	15	*f2 e c*
74885	$HgReO_4$	1/0.9/2.68	409.8	14	*e*6
28402	**$HgSO_4$**	**1/0.73/0.73**	**151.5**	**7**	*a*6
100316	**HgSO**	**1/1.01/1.38**	**151.1**	**31**	*b a4*
26985	$HoCrO_4$	1/0.88	317.1	141	*h b a*
20422	**$HoNbO_4$**	**1/2.07/0.96**	**293.6**	**5**	*c2 a2*
73392	**$HoNO_4$**	**1/2.07/0.96**	**293.3**	**15**	*f2 e2*
20409	**$HoNbO_4$**	**1/2.09/0.98**	**295.5**	**46**	*c2 b2*
35706	$HoPO_4$	1/0.88	285.4	141	*h b a*
78079	$HoVO_4$	1/0.88	319.1	141	*h b a*
100695	$InNbO_4$	1/1.12/0.94	143.5	3	*g2 f2*
16618	$InPO_4$	1/1.48/1.27	282.0	63	*g f c a*

APPENDIX—*Continued*

Col	Formula	Cell	Cell volume	SG no.	Wykoff positions
72569	$InTaO_4$	1/1.12/0.94	143.2	13	*g*2 *f e*
10431	$InVO_4$	1/1.48/1.14	324.6	63	*g f c a*
15222	$KBrO_4$	1/0.66/0.84	395.9	62	*d c*4
36152	**ClO_4**	**1/0.64/0.82**	**361.4**	**62**	*d c*4
33562	**$KClO_4$**		**416.8**	**216**	*e b a*
26964	KIO_4	1/1.55	834.8	88	*f b a*
22244	$KMnO_4$	1/0.63/0.82	386.7	62	*d c*4
1921	$KReO_4$	1/2.24	406.1	88	*f b a*
26612	$KRuO_4$	1/2.32	408.7	88	*f b a*
61	$KTcO_4$	1/2.29	407.8	88	*f b a*
20419	**$LaNbO_4$**	**1/2.03/0.92**	**339.4**	**5**	*c*2 *a*2
73390	**$LaNbO_4$**	**1/2.07/0.93**	**332.6**	**15**	*f*2 *e*2
37139	**$LaNbO_4$**	**1/2.16**	**340.5**	**88**	*f b a*
201479	**$LaPO_4$**	**1/1.03/0.95**	**303.9**	**14**	*e*6
31564	**$LaPO_4$**	**1/0.91**	**280.9**	**180**	*k d c*
20043	$LaTaO_4$	1/0.73/1.02	327.1	14	*e*6
400	$LaVO_4$	1/1.03/0.95	333.8	14	*e*6
73115	$LiMnO_4$	1/1.52/1.15	294.5	63	*g f c a*
37118	$LiReO_4$	1/0.88/0.72	520.9	2	*i* 18
2506	$LuAsO_4$	1/0.9	300.7	141	*h b a*
26988	$LuCrO_4$	1/0.88	306.1	14	*h b a*
201133	$LuPO_4$	1/0.88	274.7	141	*h b a*
20261	$LuTaO_4$	1/1.04/0.97	143.1	13	*g*2 *f e*
78083	$LuVO_4$	1/0.89	307.7	141	*h b a*
18120	**$MgCrO_4$**	**1/0.92/0.68**	**598.6**	**12**	*j*3 *i*4 *h g*
18117	**$MgCrO_4$**	**1/1.52/1.12**	**282.8**	**63**	*g f c a*
20418	$MgMoO_4$	1/0.9/0.68	641.1	12	*j*3 *i*4 *h g*
27130	**$MgSO_4$**	**1/1.81/1.41**	**272.4**	**62**	*d c*3 *a*
16759	**$MgSO_4$**	**1/1.52/1.26**	**266.1**	**63**	*g f c a*
24725	$MgUO_4$	1/1.01/1.06	297.7	74	*i h e b*
22357	$MgWO_4$	1/1.21/1.05	131.1	13	*g*2 *f e*
73489	$MnAsO_4$	1/1.34/0.72	285.3	14	*e*5 *d a*
15615	**$MnMoO_4$**	**1/0.91/0.68**	**683.1**	**12**	*j*3 *i*4 *h g*
61078	**$MnMoO_4$**	**1/1.2/1.03**	**137.7**	**13**	*g*2 *f e*
38210	$MnPO_4$	1/2.03/1.22	268.1	62	*d c*4
23839	$MnSO_4$	1/1.53/1.3	289.7	63	*g f c a*
25698	$MnSeO_4$	1/1.86/1.42	321.3	62	*d c*3 *a*
28472	$MnUO_4$	1/1.05/1.02	313.4	74	*i h e b*
15850	$MnWO_4$	1/1.19/1.03	138.4	13	*g*2 *f e*
200405	**$NaClO_4$**	**1/0.92/0.99**	**325.9**	**63**	*g f c*2
33567	**$NaClO_4$**		**381.1**	**216**	*e b a*
31428	**$NaClO_4$**		**357.9**	**225**	*j b a*
14287	$NaIO_4$	1/2.24	340.3	88	*f b a*
20583	$(Na_2U_2O_7)_{0.5}$		79.2	166	*c*2 *b a*
20407	**$SmNbO_4$**	**1/2.11/1**	**311.7**	**46**	*c*2 *b*2
201839	$SmPO_4$	1/1.03/0.95	282.4	14	*e*6
1560	$SmVO_4$	1/0.88	333.4	141	*h b a*
2748	$SnSO_4$	1/0.6/0.81	333.0	62	*d c*4
2147	**$SnWO_4$**	**1/2.07/0.89**	**327.6**	**52**	*e*2 *d c*
2840	**$SnWO_4$**		**388.8**	**198**	*b a*3
28025	$SrMoO_4$	1/2.23	349.6	88	*f b a*
31974	$SrPuO_4$		83.9	166	*c*2 *b a*
68321	**$SrSO_4$**	**1/0.64/0.82**	**309.9**	**62**	*d c*4
23744	**$SrSO_4$**		**365.5**	**216**	*e b a*
47004	$SrSeO_4$	1/1.07/1.04	348.0	14	*e*6
60507	$SrTeO_4$	1/2.35/0.89	369.6	60	*d*2 *c*2
9470	**$SrUO_4$**	**1/1.45/1.48**	**356.4**	**57**	*e d*2 *c a*
31617	**$SrUO_4$**		**84.4**	**166**	*c*2 *b a*
23701	$SrWO_4$	1/2.21	350.7	88	*f b a*

APPENDIX—*Continued*

Col	Formula	Cell	Cell volume	SG no.	Wykoff positions
20383	$TaBO_4$	1/0.88	210.5	141	*h b a*
200230	$TbAsO_4$	1/0.89	319.8	141	*h b a*
26983	$TbCrO_4$	1/0.88	323.6	141	*h b a*
35704	$TbPO_4$	1/0.87	292.3	141	*h b a*
78078	$TbVO_4$	1/0.88	325.9	141	*h b a*
201413	$TeSeO_4$	1/1.54/1.7	181.7	1	*a*12
19021	$TeVO_4$	1/3.08/1.24	321.9	14	*e*6
202081	**$ThGeO_4$**	**1/2.05**	**278.8**	**88**	*f b a*
202082	**$ThGeO_4$**	**1/0.9**	**341.8**	**141**	*h b a*
1614	**$ThSiO_4$**	**1/1.03/0.96**	**297.2**	**14**	*e*6
1615	**$ThSiO_4$**	**1/0.89**	**321.5**	**141**	*h b a*
72277	$TiNbO_4$	1/0.63	67.4	136	*f a*
72714	**$TiPO_4$**	**1/1.33/3.73**	**532.3**	**11**	*f*6 *e*12
36520	**$TiPO_4$**	**1/1.49/1.2**	**266.1**	**63**	*g f c a*
72278	$TiTaO_4$	1/0.65	68.0	136	*f a*
38392	$TiVO_4$	1/0.64	61.9	136	*f a*
65659	$TlBrO_4$	1/0.66/0.83	428.1	62	*d c*4
33564	$TlClO_4$		440.7	216	*e b a*
16619	$TlPO_4$	1/1.48/1.31	305.6	63	*g f c a*
73083	$TlReO_4$	1/3.09/2.37	1311.6	14	*e*18
36053	$TmPO_4$	1/0.88	280.0	141	*h b a*
78081	$TmVO_4$	1/0.89	312.7	141	*h b a*
15859	$UCrO_4$	1/2.42/1.04	290.1	60	*d*2 *c*2
15484	$USiO_4$	1/0.9	306.4	141	*h b a*
16492	UYO_4	1/1.02/0.95	163.2	65	*m c a*
68333	$VOSeO_3$	1/2.44/1.99	310.3	14	*e*6
36521	VPO_4	1/1.49/1.2	255.6	63	*g f c a*
9515	$VTaO_4$	1/0.65	66.4	136	*f a*
24513	$YAsO_4$	1/0.91	297.6	141	*h b a*
26989	$YCrO_4$	1/0.88	316.2	141	*h b a*
100176	$YNbO_4$	1/1.44/0.7	296.8	15	*f*2 *e*2
75127	$YO(NO_3)$	1/2.52	144.7	129	*i c*3 *a*
201131	YPO_4	1/0.87	285.0	141	*h b a*
20265	$YTaO_4$	1/1.03/0.96	147.0	13	*g*2 *f e*
78074	YVO_4	1/0.88	318.7	141	*h b a*
26987	$YbCrO_4$	1/0.88	309.7	141	*h b a*
20423	**$YbNbO_4$**	**1/2.07/0.96**	**285.9**	**5**	*c*2 *a*2
73393	**$YbNbO_4$**	**1/2.07/0.96**	**285.4**	**15**	*f*2 *e*2
20410	**$YbNbO_4$**	**1/2.08/0.98**	**288.3**	**46**	*c*2 *b*2
36054	$YbPO_4$	1/0.88	277.2	141	*h b a*
78082	$YbVO_4$	1/0.89	309.9	141	*h b a*
17030	$ZnMoO_4$	1/0.72/0.87	513.8	2	*i*18
1018	**$ZnSO_4$**	**1/0.78/0.55**	**277.1**	**62**	*d c*3 *a*
2457	$ZnSO_4$		369.5	216	*e d a*
22348	$ZnWO_4$	1/1.21/1.05	133.2	13	*g*2 *f e*
29262	$ZrGeO_4$	1/2.17	249.8	88	*f b a*
71943	$ZrSiO_4$	1/0.91	262.1	141	*h b a*
27311	$ZrTiO_4$	1/1.13/1.05	131.7	60	*d c*

REFERENCES

1. A. A. Kaminskii *Laser Crystals*: *Their Physics and Their Properties*, Chap. 1. Springer, Berlin, 1981.
2. L. Zundu and H. Yindong, *J. Phys B Condens. Matter* **6,** 3737 (1994).
3. B. G. Hyde and S. Andersson, *Inorganic Crystal Structures*, Wiley, New York, 1989.

4. L. E. Depero, C. Perego, L. Sangaletti, and G. Sberveglieri, in *Polycrystalline Thin Films*: *Structure*, *Texture*, *Properties and Applications II*, (H. J. Frost, M. A. Parker, C. A. Ross, and E. A. Holm, Eds.). MRS, Boston, 1996).
5. J. K. Burdett, *Acta Crystallogr. B* **51,** 547 (1995).
6. B. Balzer and H. Langherin, *Cryst. Res. Technol.* **31,** 93 (1996).
7. N. W. Thomas, *Acta Crystallogr. B* **52,** 16 (1996).
8. W. M. Meier and H.Villiger, *Z. Kristallogr.* **129,** 161 (1996).
9. N. Khosrovani and A. W. Sleight, *J. Solid State Chem.* **121,** 2 (1996).
10. ICSD, Inorganic Crystal Structure Database, Release 95/2, FIZ Fachinformationszentrum Karlsruhe and Gmelin-Institut.
11. The results were generated using the program CERIUS^2, developed by Molecular Simulation Incorporated.
12. A. F. Wells, *Structural Inorganic Chemistry*, Oxford Univ. Press, Oxford, 1984.
13. J. K. Burdett, *Chemical Bonding in Solids*, Oxford Univ. Press, Oxford, 1995.
14. L .E. Depero and L. Sangaletti, *J. Solid State Chem.* **119,** 428 (1995).
15. M. Kunz and I. D. Brown, *J. Solid State Chem.* **115,** 395 (1995).
16. G. D. Andreetti, G. Calestani, and A. Montenero, *J. Cryst. Growth* **71,** 289 (1985).
17. S. R. Shieh, L. C. Ming, and A. Jayaraman, *J. Phys. Chem. Solids* **57,** 205 (1996).
18. A. Jayaraman, S. Y. Wang, and S. K. Sharma, *Phys. Rev.* **B52,** 9886 (1995).
19. D. Christofilos, G. A. Kourouklis, and S. Ves, *J. Phys. Chem. Solids* **56,** 1125 (1995)
20. A. Jaraman, S. Y. Wang, S. R. Shieh, S. K. Sharma, and L. C. Ming, *J. Raman Spectrosc.* **26,** 451 (1995).
21. M. Wiesmann, H. Ehrenberg, G. Wltschek, P. Zinn, H. Weitzel, and H. Fuess, *J. Magn. Magn. Mater.* **150,** L1 (1995).